New Phytologist

Research

Noncircadian oscillations in amino acid transport have complementary profiles in assimilatory and foraging hyphae of *Phanerochaete velutina*

M. Tlalka, D. Hensman, P. R. Darrah, S. C. Watkinson and M. D. Fricker

Department of Plant Sciences, University of Oxford, South Parks Road, Oxford, OX1 3RB, UK

Author for correspondence:
M. D. Fricker
Tel: +44 (0)1865 275015
Fax: +44 (0)1865 275074
Email: mark.fricker@plants.ox.ac.uk

Received: *8 October 2002*
Accepted: *15 January 2003*

doi: 10.1046/j.1469-8137.2003.00737.x

Summary

• Cord-forming woodland basidiomycete fungi form extensive, interconnected mycelial networks that scavenge nitrogen (N) efficiently. We have developed techniques to study N dynamics in such complex mycelial systems *in vivo*.

• Uptake and distribution of the nonmetabolised, ^{14}C-labelled amino-acid analogue, α-aminoisobutyrate (^{14}C-AIB) was continuously imaged in *Phanerochaete velutina* growing across scintillation screens using an enhanced photon-counting camera.

• Oscillations in the ^{14}C-AIB signal were observed for both the assimilatory hyphae in the inoculum and the foraging hyphae, but with complementary profiles. Pulses were asymmetric, with an abrupt switch between each exponential decay phase and the next rising phase. The period of the oscillations was 16 h at 21°C, but showed a strong temperature dependence with a temperature coefficient of 2.1. Oscillations occurred in the absence of obvious pulses in growth.

• Some, but not all, of the features of the oscillations were simulated using a model of amino acid accumulation and transport that included both vacuolar uptake, and release once an intravacuolar concentration threshold was exceeded. The combination of imaging and modelling provides a useful framework to understand N fluxes *in vivo*.

Key words: *Phanerochaete velutina*, amino acid transport, vacuole, α-aminoisobutyrate, metabolic oscillations, metabolic modelling.

Introduction

Cord-forming basidiomycete fungi form extensive mycelial networks that scavenge inorganic and organic nitrogen (N) efficiently from the soil environment (Boddy & Watkinson, 1995; Dighton, 1997). Their main source of carbon (C) for respiration or provision of C-skeletons for metabolism is wood, which has very low levels of N and other nutrients, such as phosphate (Boddy & Watkinson, 1995; Dighton, 1997). Thus considerable fluxes of N and phosphorus (P) must occur from remote assimilation sites or following autolysis of redundant mycelium to regions of high demand that arise during colonization and exploitation of new wood resource (Levi & Cowling, 1969; Venables & Watkinson, 1989; Cairney, 1992; Jennings, 1994; Boddy, 1999; Olsson, 2001). Resources are often scarce, ephemeral and patchy. As a result, the mycelial network develops as a highly plastic, interconnected functional unit that continuously senses and responds to nutritional cues in the environment and translates them into developmental responses (Rayner *et al.*, 1995; Boddy, 1999; Ritz & Crawford, 1999; Olsson, 2001).

Most experimental data on nutrient transport in cord-forming mycelia is based on movement of radiolabelled phosphate (Cairney, 1992; Jennings, 1994; Boddy, 1999). There are fewer reports on N-translocation as there is no readily available radioactive N-isotope. Heavy nitrogen (^{15}N) and mass spectroscopy have been used to study transport (Arnebrant *et al.*, 1993), while stable N isotopes have proved useful in characterizing the metabolic pathways involved in mycorrhizal N metabolism using nuclear magnetic resonance (NMR) (Pfeffer *et al.*, 2001), but have not yet been applied in imaging mode to resolve N transport. An alternative strategy has been to use a ^{14}C-labelled amino-acid analogue, α-aminoisobutyric acid, (AIB) which is taken up but not

metabolised (Ogilvie-Villa *et al.*, 1981; Kim & Roon, 1982; Watkinson, 1984; Lilly *et al.*, 1990; Olsson & Gray, 1998). Because AIB is not metabolized, the ^{14}C-label faithfully reports the distribution of the amino acid analogue. Although early studies on ^{14}C-AIB translocation used destructive sampling, dynamics of ^{14}C-AIB movement were recently imaged in intact colonies of *Schizophyllum commune* using a β-scanner with spatial resolution in the order of a few millimetres and a theoretical sampling interval of about 1 h (Olsson & Gray, 1998).

To visualize N transport in mycelial networks with higher temporal and spatial resolution, we developed a novel noninvasive technique to track movement of ^{14}C-AIB in mycelia grown over an inert scintillation screen using a photon-counting camera (Tlalka *et al.*, 2002). Rapid, pulsatile movement of AIB was observed with a period of 14.5 h in growing, foraging hyphae and 11–12 h along developing cords. The oscillations were maintained for a considerable period in darkness at constant temperature.

Rhythmic phenomena are widespread in fungi and other simple eukaryotes, ranging from self-sustaining metabolic rhythms with periodicities of the order of minutes (Kippert & Hunt, 2000) to the archetypal circadian rhythms associated with sporulation in *Neurospora* (Dunlap, 1998; Ramsdale, 1999; Bell-Pedersen, 2000; Merrow *et al.*, 2001). Circadian rhythms in amino-acid uptake have been described for yeast (Edmunds *et al.*, 1979) and *Synechococcus* (Chen *et al.*, 1991). While the period of the oscillations in ^{14}C-AIB transport observed previously was clearly different from a canonical 24-h circadian rhythm, it is possible that the oscillations are tied into the output of an ultradian oscillator with a period of less than 24 hours (Dunlap, 1998; Kippert & Hunt, 2000).

In this paper we report on improvements in both the camera system and the scintillation screen that allow simultaneous measurement of signals from both assimilatory hyphae that grow on the agar inoculum and takeup nutrients from it, and distal foraging hyphae that extend over the surrounding nonnutrient area. With this more sensitive system we have tested: first, whether there are differences in the pulsatile behaviour within assimilatory and foraging hyphae; second whether the oscillations are coupled to pulses in growth; and third whether the rhythm observed is subservient to a central clock, and therefore reflects the output of that oscillator, or whether the oscillations are an intrinsic part of amino-acid uptake and translocation and may therefore yield information on the underlying control systems.

Materials and Methods

Organism

Cultures of *Phanerochaete velutina* were originally provided by Prof. L. Boddy, University of Cardiff, UK, and have been maintained in the Department of Plant Sciences, Oxford, UK, for 3 yr. Cultures were grown on 2% malt agar (2% malt extract, Oxoid Ltd, Basingstoke, UK, 2% Oxoid No. 3 agar) at 22 ± 1°C in darkness in a temperature-controlled incubator (Gallenkamp, Loughborough, UK) as previously described (Tlalka *et al.*, 2002).

Experimental microcosms

Small artificial microcosms were prepared as in Tlalka *et al.* (2002). Briefly, a submarginally cut inoculum of *P. velutina* was placed mycelial surface down in the middle of a square Petri dish on top of either a Lite Plus intensifying screen (Sigma, Poole, UK) or a BioMax TranScreen LE intensifying screen (Sigma). Humidity was maintained by the presence of water in small (500 µl) containers and by sealing the sample dishes with Parafilm (American National Can, Neenah, NI, USA). All experiments were conducted in a temperature-controlled room, usually at 21 ± 0.5°C. During experiments investigating the temperature-dependence of the oscillations the temperature was set at different values between 19°C and 26°C, as indicated in figure legends.

Visualization of ^{14}C-AIB transport using photon-counting scintillation imaging

Imaging of ^{14}C-AIB was achieved using a more sensitive version of the high-resolution, photon-counting camera system (HRPCS-3; Photek Inc., St Leonards on Sea, UK) described previously (Tlalka *et al.*, 2002). In the modified version, the three-stage microchannel-plate intensifier was equipped with a larger face-plate (40 mm diagonal) and a low-noise S20 photocathode. The larger format camera also allowed the use of higher numerical aperture photographic lenses. Data reported here used a Nikon 28 mm f/2 lens which gave a nominal (x,y) pixel dimensions of 588 µm and a field of view of 433 × 334 mm. This configuration, allowed for better reproducibility than before, because six to nine replicate experiments could be conducted in parallel with similar overall signal levels from each colony to those reported previously.

The increase in sensitivity also allowed a reduction in the amount of ^{14}C-AIB to half of that used previously. Immediately after placing the inocula on the scintillation screens, 25 µl (46.3 kBq) of a 0.9-mM solution of 2-amino[1-^{14}C]isobutyric acid, ^{14}C-AIB (Amersham, Chalfont St Giles, UK) in distilled water (specific activity 2.11 GBq mmol^{-1}) was applied to the centre of the inoculum. The chambers were then sealed and placed in continuous darkness in the camera imaging box in a temperature-controlled room. Most experiments were conducted at 21 ± 0.5°C unless otherwise stated in figure legends. The temperature within the box was continuously monitored with 'Diligence' data loggers (Comark Ltd, Stevenage, UK). Images were integrated over 30-min periods and experiments lasted for up to 480 h.

The signal from ^{14}C-AIB in assimilatory hyphae growing on the inoculum disc and foraging hyphae growing out over

the scintillation screen surface were measured simultaneously in a number of selected circular regions of interest (ROIs) of identical size (one centred on the inoculum and the others on the outwardly growing foraging hyphae). The frequency of pulses from each region was determined by Fourier analysis, essentially according to Tlalka *et al.* (2002). Briefly, total counts over 30-min periods from each region were outputted to Excel (Microsoft Corp.) and smoothed with a rolling 3- to 9-point averaging filter. Longer-term trends were eliminated by taking the second difference of each sequence (Diggle, 1990). Visual inspection indicated that this provided a reasonably stationary time-series suitable for Fourier analysis. Each series was padded with zeros to give a total of 512–2048 values to increase the resolution of the Fourier spectrum (Smith, 1997). The period of the pulses was calculated from the Fourier frequency with the greatest amplitude and the degree of synchrony assessed from the phase difference of this frequency between each region and the inoculum.

Calibration of the scintillation imaging system

To determine the sensitivity of the new camera system in combination with the new BioMax TranScreen LE intensifying screen, images were collected from a series of ^{14}C-AIB standards containing varying amounts of ^{14}C-AIB from 0 to 18.5 kBq in 20 µl droplets that had been dried on to the screen. Values of 160 photons min^{-1} nmol^{-1} ^{14}C-AIB were measured for the Lite plus screen and 1000 photons min^{-1} nmol^{-1} ^{14}C-AIB for the BioMax TranScreen LE. This compares with around 500 photons min^{-1} nmol^{-1} ^{14}C-AIB for our previous system using the Lite Plus screen (Tlalka *et al.*, 2002), but with a useable imaging area eight- to nine-fold greater than available previously. No oscillations were observed for dried-down calibration droplets imaged over 300–400 h. The increased sensitivity of the new system produced substantial file sizes during long time courses, reaching in excess of 1 GB.

To determine the level of signal from ^{14}C-AIB-loaded inoculum discs without mycelium, the signal from 25 µl of ^{14}C-AIB (46.3 kBq) was recorded from labelled agar plugs placed directly on the two different intensifying screens. The signal from the plug with mycelium was at least sevenfold higher than that simply attributable to an equivalent amount of ^{14}C-AIB allowed to equilibrate throughout an agar plug in the absence of mycelium (0.4 photons min^{-1} µm^{-2} with mycelium compared to 0.06 photons min^{-1} µm^{-2} without).

To determine the extent that the agar inoculum attenuated the signal from the hyphae growing underneath, uncolonized agar disks were randomly placed on areas of previously labelled foraging hyphae to mimic the optical path encountered by photons from ^{14}C-AIB accumulated by the assimilatory hyphae in the inoculum. Signal losses of 94% (Lite Plus) or 87.5–90% (Biomax TranScreen LE) were calculated from the ratio of ^{14}C-AIB signals from the prelabelled foraging hyphae in the presence and absence of the agar plug, after subtraction of the appropriate background.

Measurement of colony growth

The growth of colonies on the two types of intensifying screens was estimated following median filtering of the scintillation images using a 3 × 3 kernel and intensity-based thresholding to produce a segmented, binary image. The darker region corresponding to the central inoculum was included in the binary image using a hole-fill operation. Radial growth was estimated as half the maximum diameter across the segmented image following subtraction of the inoculum diameter.

In addition, the growth of *P. velutina* on the two different screens was measured under low level white-light illumination (12 W energy-saver; Osram, Münich, Germany) using time-lapse video-imaging at a photon flux of 150 µmol m^{-2} s^{-1} measured with a light power meter (model 1815-C; Newport Corp., Irvine, CA, USA). Colonies were grown under the same conditions as for the scintillation imaging except that the inoculum was loaded with either 25 µl of 0.9 mM cold AIB to match the concentration of ^{14}C-AIB, or 25 µl distilled water. Images of the growing hyphae from four replicate experiments were captured simultaneously using monochrome cameras (Cohu 4910; Brian Reece Scientific Ltd, Newburg, UK) equipped with macro zoom lenses (18–108 mm, f/2.5; Edmund Scientific, York, UK) adjusted to give field sizes of between 19 and 110 mm diagonal. Signals were digitized using a Matrox Meteor 2 framestore controlled by KCS300 software (Karl Zeiss Vision GmbH, Jena, Germany). Brightness and contrast levels were manually adjusted to achieve contrast from the fine, translucent hyphae growing across the white screens. Typically, 50 frames were averaged over 5 s to reduce noise and images collected at 30-min intervals over 250 h. Images were imported into Lucida v4.0 (Kinetic Imaging Ltd, Liverpool) and median filtered using a 3 × 3 kernel to reduce noise. The contrast for growing hyphal tips was accentuated using a high-pass filter. The linearity of growth was visualized by sampling line-transects drawn parallel to the growth direction and writing the resultant intensity plot into successive lines of a second image representing intensity along the *x*-axis and time on the *y*-axis. The rate of growth was measured as the slope of the colony profile and the uniformity of growth estimated by the linearity of the profile.

Simulation modelling of amino acid uptake and transport

Several simulation models were set up to explore the conditions under which a typical complement of amino acid transport systems and intracellular compartments might generate the observed kinetics for ^{14}C-AIB using MODELMAKER (Cherwell Scientific Publishing, Oxford, UK). Uptake of

^{14}C-AIB from the agar by assimilatory hyphae in the inoculum was assumed to operate via a saturable transport system obeying Michaelis–Menten kinetics with a K_m of 100 μM (Ogilvie-Villa *et al.*, 1981; Kim & Roon, 1982). In simulations that included a vacuolar compartment, vacuolar uptake was assumed to operate via a saturable carrier with a K_m of 400 μM (Zerez *et al.*, 1986). In addition, a vacuolar efflux system with first-order kinetics was introduced in parallel on the tonoplast that was activated once a threshold level (10 mM) of amino acid had accumulated in the vacuole. The efflux system was inactivated once the vacuolar content had fallen below a second, lower threshold set at 60% of the maximum pool size. The ^{14}C-AIB was transferred to the foraging hyphae at a rate proportional to the growth-rate, to reflect the increasing volume of the mycelium. With these constraints, the only additional variables were the apparent v_{max} for the transporters and the rate constant for the tonoplast efflux carrier. The sensitivity of the system across a range of values for each of these variables was explored. The series of interlinked differential equations were solved numerically using the fourth order Runge–Kutta method within MODELMAKER.

Movie and image presentation

Movie files were output directly from the IFS32 Imaging Software (Photek) or assembled from individual images using QuickTime Pro 4.0 (Apple Computer Inc.). Images for publication were assembled in PhotoShop 4.0 (Adobe Systems, San Jose, CA, USA).

Results

Oscillations in ^{14}C-AIB transport show complementary profiles in assimilatory and foraging hyphae

The ^{14}C-AIB was taken up by hyphae of *P. velutina* when applied to the inoculum plug and was imaged from photon emissions excited by β-particles colliding with the underlying scintillation screen. The ^{14}C-AIB signal was clearly visible in the network of foraging hyphae as the mycelium grew out across the Lite Plus (Fig. 1a) or Biomax TranScreen LE (Fig. 1b) scintillation screen. The signal was about tenfold greater from colonies on the Biomax TranScreen LE, but brightness and contrast have been normalized for both sets of images in Fig. 1. In addition, some signal was detectable from the assimilatory hyphae present under the inoculum plug itself using the more sensitive camera system in this study compared with our previous system (Tlalka *et al.*, 2002), particularly for colonies grown on the BioMax TranScreen LE (Fig. 1b). We estimate that the true signal from these hyphae was about tenfold greater, but was attenuated through absorption and/or scattering by the agar plug (see the Materials and Methods).

The scintillation signal from the assimilatory hyphae rose rapidly to a maximum around 50–100 h after the addition of ^{14}C-AIB, with virtually no detectable lag (Fig. 1c,d). Following this initial increase, the overall signal from this region slowly declined to a lower plateau over the next 50–100 h. The signal intensity from a similar-sized region of foraging hyphae adjacent to the inoculum increased after 30–40 h as the foraging hyphae grew out across the measurement area, with the signal typically reaching a maximum around 150–200 h, depending on the precise colony morphology.

Low-amplitude oscillations were superimposed on the long-term trends for both foraging and assimilatory hyphae (Fig. 1c,d). The oscillations had similar frequency for both types of hyphae, but showed complementary profiles, even though the regions measured were within a few millimetres of each other (Fig. 1a,b). This was seen more clearly once the longer-term trends were removed by taking the second-order difference of the time-series (Fig. 1e,f). The oscillations from the assimilatory and foraging hyphae followed the same overall envelope, increasing in amplitude up to around 100 h then decaying slowly, but were almost perfectly syncopated. Fourier analysis confirmed that the dominant frequency was the same for both sets of oscillations and was similar between colonies growing on the two types of screen (Fig. 1g,h). The corresponding period of the oscillations at 21°C was around 16 h (Table 1).

Oscillations are asymmetric

Closer inspection of the oscillations revealed that they were not sinusoidal, but showed a pronounced asymmetry that was particularly apparent once the plateau phase was reached in colonies grown over the Biomax TranScreen LE (Fig. 2). In the foraging hyphae, there was a slow rise lasting around 11 h during the first phase (P1) of the cycle, followed by an abrupt switch to rapid decay lasting about 5 h in the second phase (P2) of the cycle (Fig. 2 and Table 1). The opposite pattern was observed for the assimilatory hyphae, starting with a slow, exponential-like drop and followed by a rapid recovery. This asymmetry was reflected in the Fourier analysis that showed additional peaks in the spectrum, notably at the first harmonic (Fig. 1g,h).

Oscillations are not tightly linked to an internal clock

Colonies were exposed to a short (1 h) light break before transfer to continuous darkness for the imaging experiments. There was no evidence that this pretreatment was sufficient to entrain the subsequent oscillations as pulses recorded from mycelia in replicate experiments conducted simultaneously in the same chamber were not synchronized (Fig. 3a). The lack of synchrony also rules out the possibility that oscillations were associated with cyclical changes in environmental conditions or instrument artefacts.

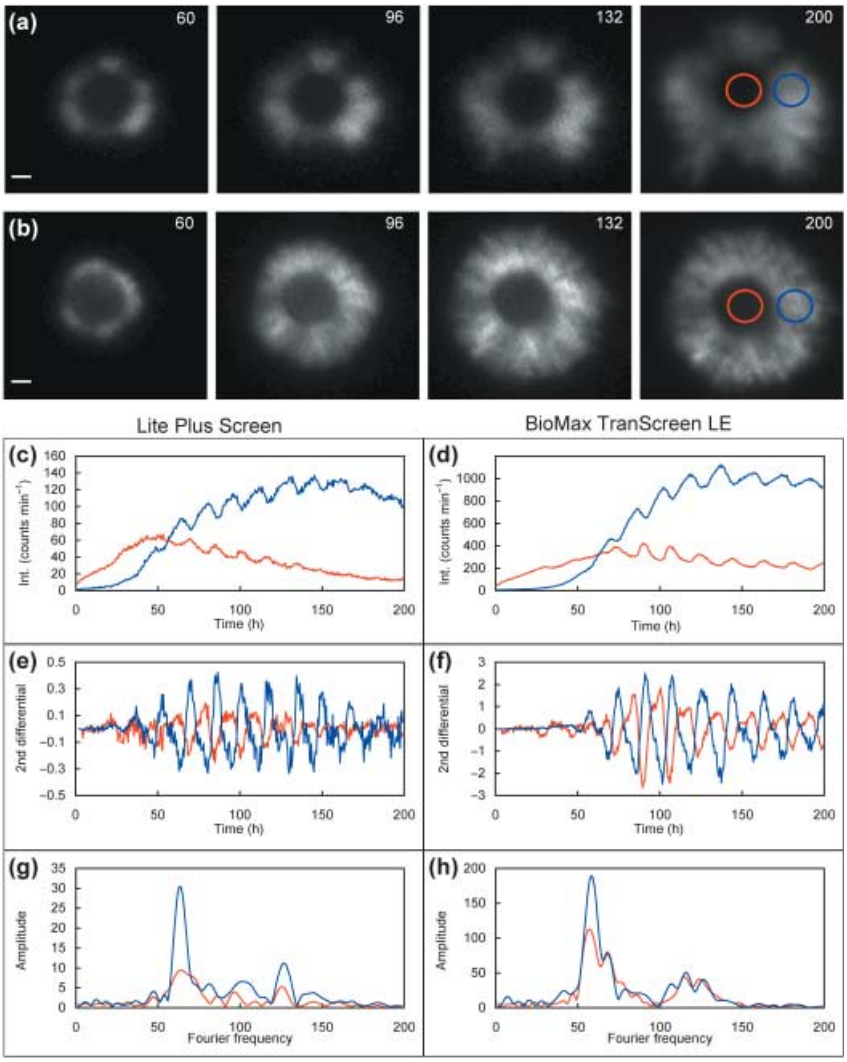

Fig. 1 Complementary oscillations of ^{14}C-labelled α-aminoisobutyrate (^{14}C-AIB) in assimilatory and foraging hyphae of *Phanerochaete velutina.* The distribution of ^{14}C-AIB was mapped using photon-counting scintillation imaging of colonies of *P. velutina* grown across Lite Plus (a) or Biomax TranScreen LE (b). Four images, each integrated over 30 min, are shown for the times indicated from a complete time-series lasting over 200 h. In addition to the strong ^{14}C-AIB signals observed in the foraging mycelia, weaker signal were also detected in the assimilatory hyphae underlying the inoculum plug. The total signal, measured for regions of comparable size for assimilatory (red) and foraging hyphae (blue), showed pronounced oscillations for colonies grown on either type of screen (c,d). The oscillations showed complementary profiles between the assimilatory and foraging hyphae. This was most clearly seen after the longer-term trends were removed by taking the second difference of the time series (e,f). The maximum Fourier frequency of these sequences was around 58–63, corresponding to a period of 16.25 h (Lite Plus) and 17.6 h (BioMax TranScreen LE) for both the assimilatory and foraging hyphae. Additional peaks were present in the Fourier spectrum at higher harmonics of the fundamental frequency. These reflect the underlying asymmetry in the shape of each pulse. Bars, 10 mm.

Table 1 Characteristics of oscillations in ^{14}C-labelled α-aminoisobutyrate (^{14}C-AIB) levels in foraging mycelia of *Phanerochaete velutina*

	Lite Plus	BioMax TranScreen LE
Period[1]	15.9 ± 0.8 (*n* = 12)	15.9 ± 1.7 (*n* = 6)
Duration of the first phase of the cycle (P_1)[2]	11.1 ± 1.9 (*n* = 8)	11.8 ± 0.8 (*n* = 12)
Duration of the second phase of the cycle (P_2)[2]	5.5 ± 0.8 (*n* = 8)	4.9 ± 0.8 (*n* = 12)

[1]Values are given as the mean ± SD, with the number of separate experiments given in brackets. [2]Values are given as the mean ± SD. The total number of well-defined peaks measurable from the plateau phase from six separate experiments is given. Typically one to three peaks were analysable per experiment.

To investigate the temperature dependence of oscillations further in this study, the period was measured using Fourier analysis from foraging hyphae grown at a range of different temperatures between 19°C and 25.5°C. The period decreased markedly with increasing temperature (Fig. 3b). The temperature coefficient (Q_{10}) was calculated as 2.1 by extrapolation from the ratio of the frequency at a given temperature to the frequency at a temperature 10°C higher (Fig. 3b, inset). In several of these experiments, colonies were also shifted between temperatures. The period of the oscillations adjusted to the temperature within a few cycles but there was no evidence that the phase of the oscillation was reset by the temperature jump (data not shown). The timing of the temperature jump differed with respect to the phase of the cycle in parallel colonies, but, in the absence of clear support for an underlying circadian or ultradian rhythm, we have not systematically

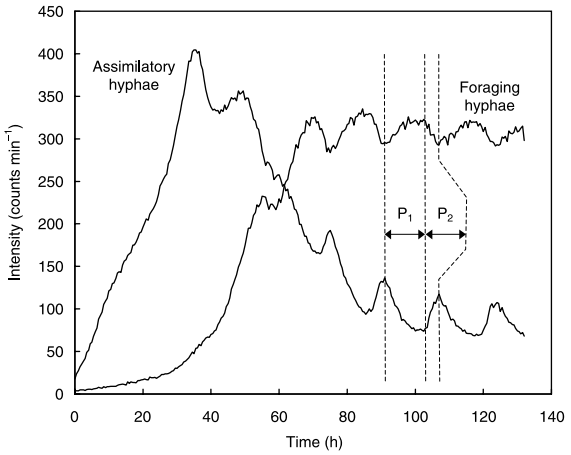

Fig. 2 Oscillations exhibit two distinct phases in each cycle. Oscillations in ^{14}C-labelled α-aminoisobutyrate (^{14}C-AIB) signal were not symmetrical particularly during the plateau after around 80–100 h. The first phase of each cycle (P_1) in the foraging hyphae showed an initial rapid rise tailing off to a plateau, followed by an abrupt switch to an exponential decay in the second phase of the cycle (P_2). The reverse was observed for the assimilatory hyphae, with an exponential decay in the first part of the cycle followed by an abrupt switch to rapid accumulation in the second phase.

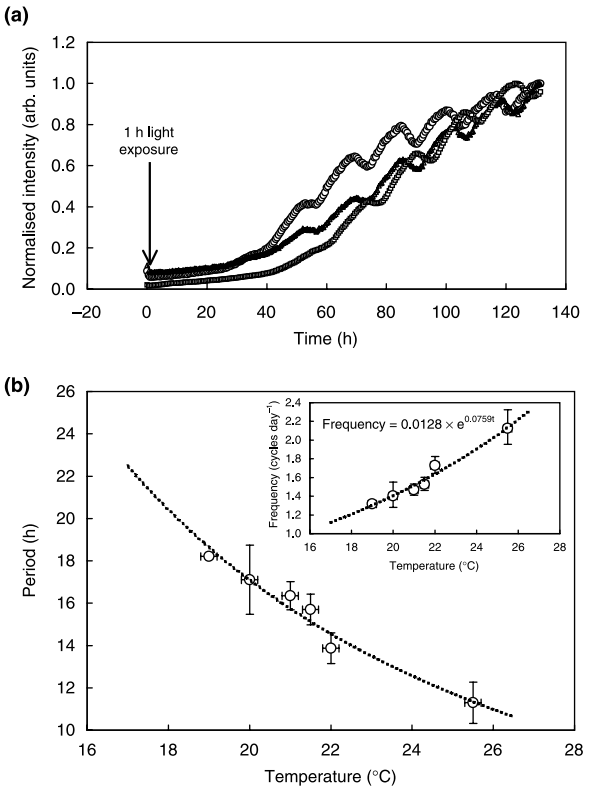

Fig. 3 Oscillations are not linked to an underlying clock. Six replicate colonies were exposed to a short (1 h) light break at the start of imaging and then maintained in darkness at constant (21 ± 0.5°C) temperature. This light break did not entrain the subsequent oscillations. Three representative traces are shown in (a). The temperature dependence of the oscillation period was measured using Fourier analysis when the whole apparatus was maintained at varying temperatures between 19°C and 26°C in a temperature-controlled room. The period decreased markedly with increasing temperature (b). The temperature coefficient (Q_{10}) was calculated from the corresponding frequency (inset) and gave a value of 2.1.

tested whether temperature jumps or light breaks could entrain the rhythm at defined phases of the cycle.

Radial growth of the colony does not have a clear pulsatile component

To test whether the pulses of ^{14}C-AIB detectable in the foraging hyphae were associated with periodic changes in growth rate or growth habit, the colony diameter was estimated following intensity-based thresholding of the scintillation images. On both screens, growth was relatively slow for the first 30–40 h then increased to a maximum around 70–100 h before tailing off again by 200 h (e.g. Fig. 4a). The apparent growth, determined as the maximum colony diameter, was greater for colonies grown on the Biomax TranScreen compared with the Lite Plus (Table 2). However, these figures are slightly misleading because part of the apparent difference in growth arises from stochastic variations in colony morphology. Radially symmetrical colonies (Fig. 4b) had a lower diameter than those where symmetry was broken (e.g. Fig. 4c). These measurements of growth can provide only a crude descriptor of the true colony behaviour.

No obvious oscillations or pulsatile surges in growth were observed in the segmented scintillation images. It is possible that the inherent noise in the images led to quite large variance in the estimate of colony diameter at successive time points (e.g. Fig. 4a) that might have obscured subtle fluctuations in growth. To achieve more precise visualization of growth behaviour, colonies growing across scintillation screens were imaged under bright-field conditions. As the scintillation experiments were conducted in darkness, we first ascertained that growth of *P. velutina* (on agar) was not markedly affected by light intensity up to 150 μmol m^{-2} s^{-1} – the highest intensity tested (Table 2) – and showed little or no dependence on wavelength (data not shown). Over the first 70–100 h growth was mainly in the form of relatively infrequently branched thin hyphae growing on or near the surface of the screen. There was no detectable pulsatile component for growth during this period whether colonies were grown on agar or on scintillation screens and in the presence or absence of cold AIB (Fig. 4d–f and Table 2). From this point forward, colony growth became progressively more complex. Radial expansion continued at roughly the same rate but branching became more frequent, some hyphae appeared to regress and the initial radial symmetry altered in favour of a more limited number of discrete point growth foci (compare Fig. 4b,c) typical of the early stages in development of a corded system. There was no obvious synchronization of these events throughout the colony with a

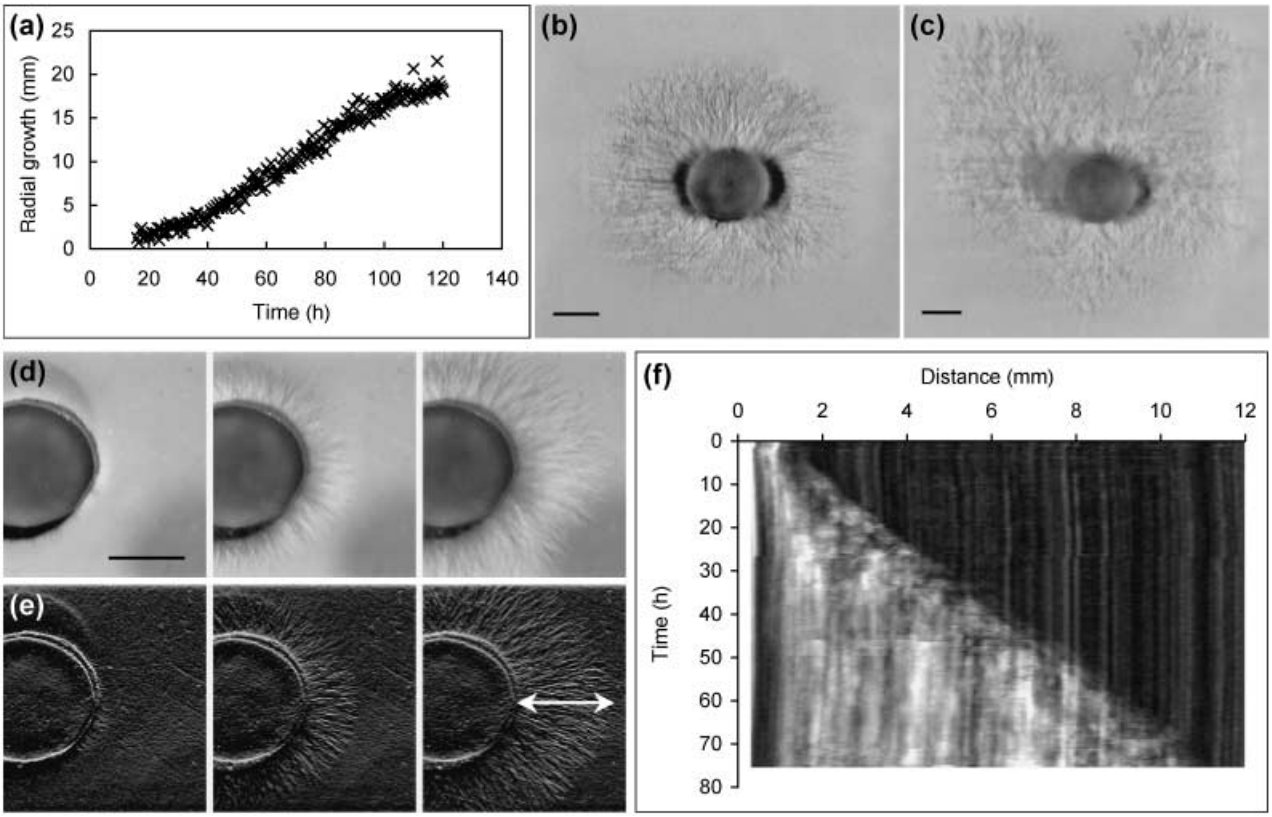

Fig. 4 Measurement of colony growth from scintillation images and bright-field images. Growth was estimated as the change in radius across an intensity-thresholded scintillation image (a). No obvious cyclical changes in growth were detected that corresponded to the periodicity observed in the ^{14}C-labelled α-aminoisobutyrate (^{14}C-AIB) measurements. Bright-field images at the end of the scintillation imaging experiments (b,c) revealed that colony growth was not necessarily uniform with local regions of increased branching and growth from discrete foci typical of the early stages of cord formation. Higher resolution of colony growth patterns was achieved using time-lapse bright-field imaging (d). Contrast was very low for the fine, white hyphae growing over a white screen so images were processed using a high-pass filter (e) to give greater contrast. The profile for growth of the colony margin was visualized from the transect indicated in (e) and is presented as a length–time plot (f). Growth was linear over at least 70 h, with no obvious pulsatile component. Bar, 10 mm.

Table 2 Growth of *Phanerochaete velutina* on different substrates

Substrate	AIB[1]	Light	Measurement technique	Maximum growth rate[2] (μm h^{-1})
Agar	–	–	Direct measurement	238 ± 14 (*n* = 12)
Agar	–	+	Direct measurement	211 ± 17 (*n* = 12)
BioMax TranScreen	+	–	Scintillation imaging	317 ± 66 (*n* = 6)
Lite Plus	+	–	Scintillation imaging	186 ± 72 (*n* = 12)
Lite Plus	+	+	Bright-field image analysis	157 ± 39 (*n* = 4)
Lite Plus	–	+	Bright-field image analysis	168 ± 12 (*n* = 4)

[1]AIB, α-aminoisobutyrate. [2]Values are given as the mean ± SD, with the number of separate experiments given in brackets.

periodicity that might be associated with oscillations in ^{14}C-AIB transport. However, we cannot rule out subtle changes in growth pattern due to the technical difficulties of imaging morphological changes within the mass of thin, white hyphae superimposed on the white scintillation screen. For example, we might not detect cycles where a limited number of unsuccessful foraging hyphae regress and their contents are remobilized to support growth at the margin.

Discussion

^{14}C-AIB is taken up rapidly by the assimilatory hyphae in the inoculum

The improved sensitivity of the camera system used in this study compared with our previous system (Tlalka *et al.*, 2002) enabled simultaneous measurement of ^{14}C-AIB dynamics for

hyphae performing different physiological roles, namely nutrient uptake by assimilatory hyphae in the inoculum and exploratory growth by the foraging hyphae. The assimilatory hyphae growing under the inoculum plug accumulated ^{14}C-AIB avidly from a relatively low concentration (22 μM), presumably through the action of a plasma membrane amino acid transporter(s). In fungi, including saprotrophic basidiomycetes (e.g. Kersten *et al.*, 1999), a range of amino acid uptake systems exist in parallel on the plasma membrane, including high-affinity transporters for specific amino acids with K_m values in the 1–1000 μM range, and more general amino acid permeases with slightly lower affinities (Horák, 1997; Chalot & Brun, 1998). These transporters share homology with members of amino acid transporter families described for animals and plants (Wipf *et al.*, 2002). Although AIB most closely resembles the neutral amino acid alanine in structure, uptake experiments suggest that it may be transported by a general amino acid permease in both *Neurospora* (Olgilvie-Villa *et al.* 1981) and *Sacharomyces* (Kim & Roon, 1982) with K_m values of 98.7 μM and 270 μM, respectively. The situation in basidiomycetes is not yet resolved with the limited data available from competition studies. Thus, AIB uptake is inhibited by high levels of glutamate in *Serpula lacrymans* (Watkinson, 1984) or L-asparagine in *Schizophyllum commune* (Lilly *et al.*, 1990). These amino acids are likely to be taken up both by a general amino acid permease and by more specific transporters. Apparently nonsaturable uptake systems may also contribute to assimilation of some amino acids (Chalot & Brun, 1998; Anderson *et al.*, 2001), although these typically operate at higher substrate concentrations than those used here. The absence of a detectable lag period in uptake (Fig. 1c,d) suggests that the transporter(s) was already present in the membrane rather than requiring induction and *de novo* expression.

Asymmetric oscillations highlight physiological differences between assimilatory and foraging hyphae

Following uptake, ^{14}C-AIB was distributed to the foraging hyphae growing out from the inoculum. Asymmetric oscillations were observed for both the assimilatory and foraging hyphae with complementary profiles. It is difficult to infer the underlying mechanisms that would generate such asymmetrical pulses, particularly the sharp transitions between the two apparently distinct phases of the cycle. We can exclude a tight coupling to an ultradian/circadian clock as, although the oscillations persisted in constant conditions, they showed a marked temperature dependence. Similarly, we have not been able to detect synchronized changes in marginal growth that might drive cyclical changes in flux, although we cannot rule out more subtle cycles of regression and redistribution within the foraging hyphae. Even if such morphological changes did occur, it is not immediately apparent how the complementary profile of the rhythm in the assimilatory and foraging hyphae and the distinct switch in behaviour during the cycle would be generated. Previously (Tlalka *et al.*, 2002) we suggested that cyclical changes in the fungal structure or local distribution of ^{14}C-AIB might alter the efficiency with which photons were either generated or detected and thus generate artefactual pulses. This explanation now seems less likely, unless the underlying process also operates asynchronously in the assimilatory and foraging hyphae. We have therefore focused on physiological and biochemical explanations of the pulsing behaviour.

Oscillatory behaviour can be simulated with a pool-refilling model

To link the *in vivo* observations in this study with existing biochemical information, we developed a simulation model that included saturable AIB uptake across the plasma membrane, followed by distribution throughout the mycelium by a mass-flow mechanism (Fig. 5a). Because there is also extensive evidence that fungi accumulate amino acids in their vacuoles under conditions of high N-availability (Kitamoto *et al.*, 1988; Watkinson, 1999), vacuolar transport was also included in the simulation. Although vacuolar uptake may be mediated by both high-affinity (Zerez *et al.*, 1986) and low-affinity (Keenan & Weiss, 1997) tonoplast amino-acid transporters (Klionsky *et al.*, 1990; Horák, 1997; Wipf *et al.*, 2002), only a single saturable tonoplast transport system was included in the model. The kinetic parameters for the transporters and the constants used in the simulation are given in Fig. 5b.

Under conditions of N demand, stored vacuolar amino acids are mobilized and there is growing biochemical and molecular evidence for the involvement of a specific set of tonoplast efflux transporters (Keenan & Weiss, 1997; Russnak *et al.*, 2001). Molecular insights into control of the switch between accumulation and release are also beginning to emerge, particularly from studies on selective permeabilization of the plasma membrane to allow direct access to the tonoplast (Keenan & Weiss, 1997; Roos *et al.*, 1997). While vacuolar amino acid uptake appears to be independent of the intravacuolar concentration, efflux is initiated immediately vacuolar amino acid levels exceed a threshold value (Keenan & Weiss, 1997; Roos *et al.*, 1997). The consequences of such a system operating were explored in the simulation. In permeabilized cell models, efflux is also stimulated by changes in the cytoplasmic nucleotide pools (Roos *et al.*, 1997; Steighardt *et al.*, 2000), but this level of control has not yet been incorporated into the model.

In the simulation, the plasma membrane uptake step alone, in the absence of vacuolar transport, was not capable of generating oscillations, even if feedback-inhibition by increasing cytoplasmic concentrations was included in the model (Fig. 5c). Similarly, inclusion of a vacuolar compartment yielded a greater net accumulation in the assimilatory hyphae, but did

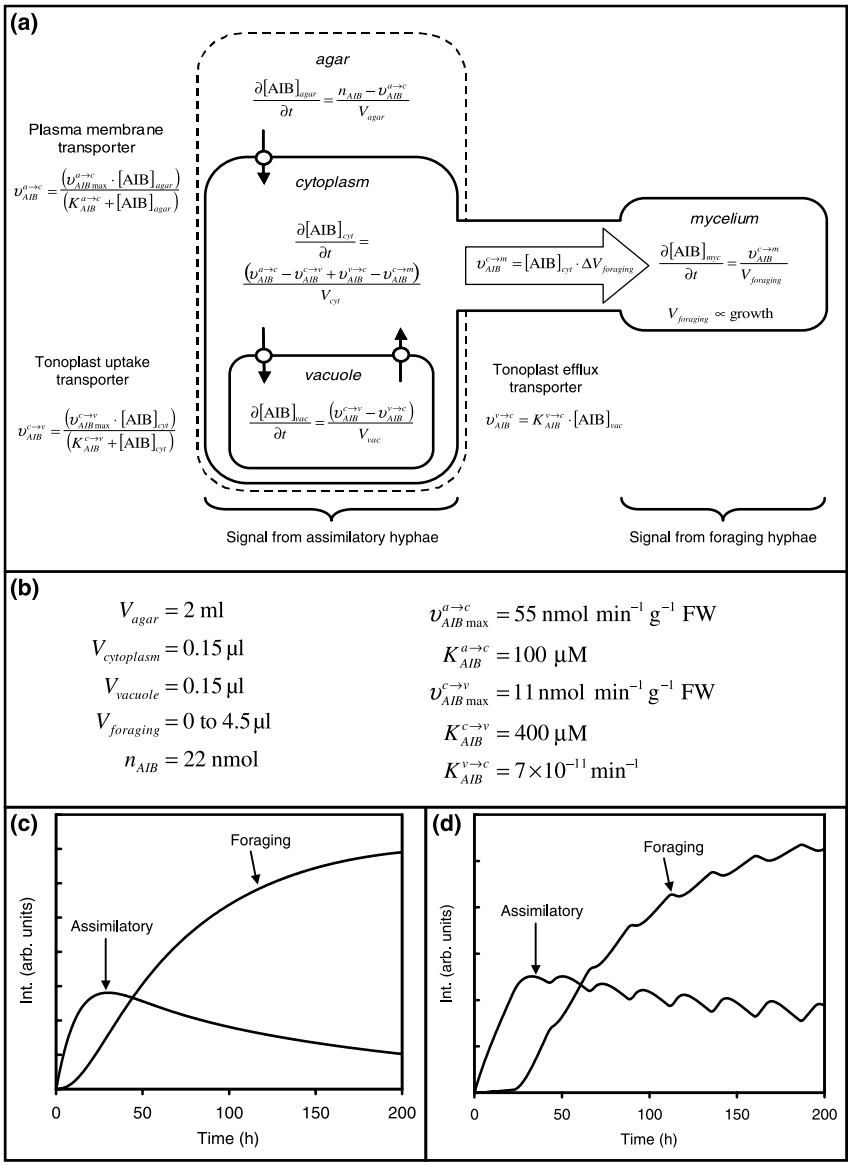

Fig. 5 Simulation for generating oscillations based on a vacuolar pool refilling model. The ^{14}C-labelled α-aminoisobutyrate (^{14}C-AIB) dynamics were modelled as the interaction between fluxes across the plasma membrane and tonoplast in the assimilatory hyphae and transport to the foraging hyphae (a). Uptake across the plasma membrane and tonoplast were modelled using Michaelis–Menten kinetics, using apparent K_m values drawn from the literature (b). Efflux from the vacuole was modelled with first-order kinetics that were triggered once the intravacuolar concentration reached a threshold level. Efflux was shut down once the intravacuolar concentration had fallen to 60% of its maximum value. Translocation to the foraging hyphae was modelled at a rate proportional to the growth of the mycelium measured experimentally and the cytoplasmic concentration. Superscripts refer to the compartment as follows: c, cytoplasm; a, agar; v, vacuole; the direction of the arrow indicates the direction of the flux. The output of the model for similar sized areas of assimilatory and foraging mycelium is shown in (c) for the case with no vacuolar transport, and in (d) for the full model. The combination of cyclical uptake and release from the vacuole and continuous removal to the foraging hyphae was sufficient to simulate several of the features observed in the *in vivo* imaging experiments.

not give rise to oscillations (data not shown). However, the type of hysteresis required to generate a continuous train of pulses was observed if a threshold-dependent transition between uptake and release from the vacuolar storage pool was included (Fig. 5d). In this simulation, uptake into the vacuolar storage pool was allowed to proceed through a saturable carrier with a K_m of 400 µM (Zerez *et al.*, 1986) and efflux was via a system with first-order kinetics, which was activated once a threshold level of amino acid accumulated in the vacuole. The efflux system was inactivated once the vacuolar content fell below a second, lower threshold, set at 60% of the maximum pool size. A range of values for each of the variables were explored (the results shown in Fig. 5d are illustrative). This combination of cyclical uptake and release from the vacuole plus continuous removal to the foraging hyphae was sufficient to simulate several of the major features observed *in vivo*, including the rapid increase in signal in the assimilatory hyphae, the delayed increase in signal from the foraging hyphae and the superimposed complementary asymmetric oscillations.

It is encouraging that a relatively simplistic model using generic components provides a reasonable description of the pulsatile behaviour in an intact system. If validated by further work, it suggests that the combination of *in vivo* analysis and simulation modelling might prove a useful route to understand the control of fluxes between the cytoplasmic and vacuolar amino acid pools operating *in vivo*. Equally, we cannot rule out, at this stage, that pulses are generated by a more complex series of control systems involving a greater number of compartments and/or differentiated hyphae.

Are the observed oscillations unique to rapid ^{14}C-AIB exposure?

While such simulations may highlight the importance of coordination between transport and vacuolar storage in amino acid homeostasis, a number of important caveats remain. First, it might be expected that if the sudden uptake of readily-available amino acid exceeds throughput to the rest of the mycelium, the system will be prone to oscillate (Rayner *et al.*, 1995). The oscillations would then map the trajectory of the displaced system as it returns to its unperturbed state rather than highlight an intrinsic regulatory feature of N uptake and translocation in this fungus.

It should be noted that AIB is also not without biological effect. The extent that AIB interferes with normal N-sensing and metabolism is not well established. At high (mM) concentrations, AIB suppresses exploratory growth, tricking the fungus into an assimilatory growth pattern by inhibiting cord development and hyphal extension and increasing branch frequency (Elliot & Watkinson, 1989), even though AIB cannot be metabolized (Watkinson, 1984). It is possible that AIB may directly interfere with external N-sensing systems at the plasma membrane, such as a homologue of amino acid sensing permease, Ssy1p (reviewed by Gagiano *et al.*, 2002), or disturb intracellular N sensing by competing for transporters or energy gradients involved in maintaining normal amino acid pool sizes. If this were to impact on the level of glutamine, for example, it might perturb intracellular N sensing through interactions of uncharged glutamine $tRNA_{CUG}$ molecules with a kinase cascade (reviewed by Gagiano *et al.*, 2002). Alternatively, because AIB is not metabolized, it may not be recognized by the normal regulatory control mechanisms, and consistently overshoot the normal homeostatic set points.

Evidence from yeast indicates that AIB may act as an effector of N catabolite repression in the presence of poor nitrogen sources, but not with good N sources (Kim & Roon, 1982). Whether this is a specific effect is less clear, as the concentrations used (1–10 mM) were also sufficient to inhibit protein synthesis (Kim & Roon, 1982). The external concentration of AIB used here (22 μM) was significantly lower than this and did not affect the growth of *Phanerochaete* in this study. In our previous report (Tlalka *et al.*, 2002), we attributed the reduction in growth observed after several days to the presence of AIB. It now seems more likely that the major effect on growth was the higher temperatures (up to 26°C) that arose during the imaging experiments with the previous camera system.

Any inhibitory effects of AIB may also be masked by the high levels of other amino-acids in the relatively rich malt agar inoculum used. It will be interesting in future work to bring the overall AIB : N ratio under experimental control to see if it is possible to directly correlate changes in growth pattern with the intracellular N status throughout the entire, intact foraging mycelial network.

In summary, oscillations in ^{14}C-AIB uptake and transport were not associated with a circadian or ultradian rhythm in *P. velutina*, but showed a marked temperature-dependence consistent with a self-sustaining metabolic rhythm. We infer from the asymmetric shape of the pulses, particularly the abrupt transition between each exponential decay phase and the next rising phase, that a switch-like phenomenon takes place in the underlying uptake and transport systems. A model that included known properties of transporters in other fungal systems and sequestration/release from the vacuole simulated several aspects of the observed behaviour, including the complementary profiles of the pulses in the assimilatory and foraging hyphae. This model focuses attention on the possible role of vacuolar uptake and release of amino acids as a regulatory step in the pathway of N from outside the cell into intracellular metabolism, and may, in future, help us in the investigation of the morphogenetic effect of nutrients that is such a striking feature of fungal development. It is well established that facultative development of multihyphal aggregated structures responds to external nutrient triggers and available evidence (reviewed by Watkinson, 1999) implicates intracellular amino acid levels in the signalling pathway.

Acknowledgements

We gratefully acknowledge financial support from the Natural Environment Research Council (grant no. GR3/12946) and from the Dunstan Bequest (University of Oxford).

References

Anderson IC, Chambers SM, Cairney JWG. 2001. Characteristics of glutamate uptake by two Australian *Pisolithus* species. *Mycological Research* **105**: 977–982.

Arnebrant K, Ek H, Finlay RD, Söderström B. 1993. Nitrogen translocation between *Alnus glutinosa* (L.) Gaertn. Seedlings inoculated with *Frankia* sp. and *Pinus contorta* doug. Es Loud seedlings connected by a common ectomycorrhizal mycelium. *New Phytologist* **124**: 231–242.

Bell-Pedersen D. 2000. Understanding circadian rhythmicity in *Neurospora crassa*: from behaviour to genes and back again. *Fungal Genetics and Biology* **29**: 1–18.

Boddy L. 1999. Saprotrophic cord-forming fungi: meeting the challenge of heterogeneous environments. *Mycologia* **91**: 12–32.

Boddy L, Watkinson SC. 1995. Wood decomposition, higher fungi, and their role in nutrient redistribution. *Canadian Journal of Botany* **73**: S1377–S1383.

Cairney JWG. 1992. Translocation of solutes in ectomycorrhizal and saprotrophic rhizomorphs. *Mycological Research* **96**: 135–141.

Chalot M, Brun A. 1998. Physiology of organic nitrogen acquisition by ectomycorrhizal fungi and ectomycorrhizas. *FEMS Microbiology Reviews* **22**: 21–44.

Chen T-H, Chen T-L, Hung L-M, Huang T-C. 1991. Circadian rhythms in amino acid uptake by *Synechococcus* RF-1. *Plant Physiology* **97**: 55–59.

Diggle PJ. 1990. *Time series, a biostatistical introduction. Oxford Statistical Science Series.* Oxford, UK: Clarendon Press.

Dighton J. 1997. Nutrient cycling by saprotrophic fungi in terrestrial habitats. In: Wicklow DT, Söderström B, eds. *The Mycota IV:*

environmental and microbial relationships. Berlin, Germany: Springer-Verlag, pp. 271–279.

Dunlap JC. 1998. Common threads in eukaryotic circadian systems. *Current Opinion in Genetics and Development* **8**: 400–406.

Edmunds LN Jr, Apter RI, Rosenthal PJ, Shen WK, Woodward JR. 1979. Light effect in yeast: persisting oscillations in cell division activity and amino acid transport in cultures of *Saccharomyces cerevisiae* entrained by light–dark cycles. *Photochemistry and Photobiology* **30**: 595–601.

Elliot ML, Watkinson SC. 1989. The effect of α-aminoisobutyric acid on wood decay and wood spoilage fungi. *International Biodeterioration* **25**: 355–371.

Gagiano M, Bauer FF, Pretorius IS. 2002. The sensing of nutritional status and the relationship to filamentous growth in *Saccharomyces cerevisiae*. *FEMS Yeast Research* **1502**: 1–38.

Horák J. 1997. Yeast nutrient transporters. *Biochimica et Biophysica Acta* **1331**: 41–79.

Jennings DH. 1994. Translocation in mycelia. In: Wessels JGH, Meinhardt H, eds. *The Mycota I: growth, differentiation and sexuality*. Berlin, Germany: Springer-Verlag, 163–173.

Keenan KA, Weiss RL. 1997. Characterisation of vacuolar arginine uptake and amino acid efflux in *Neurospora crassa* using cupric ion to permeabilise the plasma membrane. *Fungal Genetics and Biology* **22**: 177–190.

Kersten MASH, Arninkhof MJC, Op den Camp HJB, van Griensven LJLD, van der Drift C. 1999. Transport of amino acids and ammonium in mycelium of *Agaricus bisporus*. *Biochimica et Biophysica Acta* **1428**: 160–272.

Kim KW, Roon RJ. 1982. Transport and metabolic effects of α-aminoisobutyric acid in *Saccharomyces cerevsiae*. *Biochimica et Biophysica Acta* **719**: 356–362.

Kippert F, Hunt P. 2000. Ultradian clocks in eukaryotic microbes: from behavioural observation to functional genomics. *Bioessays* **22**: 16–22.

Kitamoto K, Yoshizawa K, Ohsumi Y, Anraku Y. 1988. Dynamic aspects of vacuolar and cytosolic amino acid pools of *Saccharomyces cerevisiae*. *Journal of Bacteriology* **170**: 2683–2686.

Klionsky DJ, Herman PK, Emr SD. 1990. The fungal vacuole: composition, function and biogenesis. *Microbiological Reviews* **54**: 266–292.

Levi MP, Cowling EB. 1969. Role of nitrogen in wood deterioration VII. Physiological adaptation of wood destroying fungi and other fungi to substrates deficient in nitrogen. *Phytopathology* **59**: 460–468.

Lilly WW, Higgins SM, Wallweber GJ. 1990. Uptake and translocation of 2-aminoisobutyric acid by *Schizophyllum commune*. *Experimental Mycology* **14**: 169–177.

Merrow M, Roenneberg T, Macino G, Franchi L. 2001. A fungus among us: the *Neurospora crassa* circadian system. *Seminars in Cell and Developmental Biology* **12**: 279–285.

Ogilvie-Villa S, DeBusk RM, DeBusk AG. 1981. Characterisation of 2-aminoisobutyric acid transport in *Neurospora crassa*: a general amino acid permease-specific substrate. *Journal of Bacteriology* **147**: 945–948.

Olsson S. 2001. Colonial growth of fungi. In: Howard RJ, Gow NAR, eds. *The Mycota VIII: biology of the fungal cell*. Berlin, Germany: Springer-Verlag, 125–141.

Olsson S, Gray SN. 1998. Patterns and dynamics of ^{32}P-phosphate and labelled 2-aminoisobutyric acid (^{14}C-AIB) translocation in intact basidiomycete mycelia. *FEMS Microbiology Ecology* **26**: 109–120.

Pfeffer PE, Bago B, Shachar-Hill Y. 2001. Exploring mycorrhizal function with NMR spectroscopy. *New Phytologist* **150**: 543–553.

Ramsdale M. 1999. Circadian rhythms in filamentous fungi. In: Gow NAR, Robson GD, Gadd GM, eds. *The fungal colony*. Cambridge, UK: Cambridge University Press, 75–107.

Rayner ADM, Griffith GS, Ainsworth AM. 1995. Mycelial interconnectedness. In: Gow NAR, Gadd GM, eds. *The growing fungus*. London, UK: Chapman & Hall, 21–40.

Ritz K, Crawford JW. 1999. Colony development in nutritionally heterogeneous environments. In: Gow NAR, Robson GD, Gadd GM, eds. *The fungal colony*. Cambridge, UK: Cambridge University Press, 49–74.

Roos W, Schulze R, Steighardt J. 1997. Dynamic compartmentation of vacuolar amino acids in *Penicillium cyclopium*. *Journal of Biological Chemistry* **272**: 15849–15855.

Russnak R, Konczal D, McIntire SL. 2001. A family of yeast proteins mediating bi-directional vacuolar amino acid transport. *Journal of Biological Chemistry* **276**: 23849–23857.

Smith SW. 1997. *The scientist and engineer's guide to digital signal processing*. San Diego, CA, USA: Technical Publishing.

Steighardt J, Meyer K, Roos W. 2000. Selective regulatory effects of purine and pyrimidine nucleotides on vacuolar transport of amino acids. *Biochimica et Biophysica Acta* **1497**: 321–327.

Tlalka M, Watkinson SC, Darrah PR, Fricker MD. 2002. Continuous imaging of amino-acid transport in intact mycelia of *Phanerochaete velutina* reveals rapid, pulsatile fluxes. *New Phytologist* **153**: 173–184.

Venables CE, Watkinson SC. 1989. Medium-induced changes in patterns of free and combined amino acids in mycelium of *Serpula lacrimans*. *Mycological Research* **92**: 273–277.

Watkinson SC. 1984. Inhibition of growth and development of *Serpula lacrimans* by the nonmetabolised amino acid analogue α-aminoisobutyric acid. *FEMS Microbiology Letters* **24**: 247–250.

Watkinson SC. 1999. Metabolism and hyphal differentiation in large basidiomycete colonies. In: Gow NAR, Robson GD, Gadd GM, eds. *The fungal colony*. Cambridge, UK: Cambridge University Press, 127–157.

Wipf D, Ludewig U, Tegeder M, Rentsch D, Koch W, Frommer WB. 2002. Conservation of amino acid transporters in fungi, plants and animals. *Trends in Biochemical Sciences* **27**: 139–147.

Zerez CR, Weiss RL, Franklin C, Bowman BJ. 1986. The properties of arginine transport in vacuolar membrane vesicles of *Neurospora crassa*. *Journal of Biological Chemistry* **261**: 8877–8882.